Photo-Induced Electron Transfer from Excited Tris[2,2′-bipyridine-κN^1,$\kappa N^{1'}$]ruthenium(2+) Ions to Dyadic Electron Acceptors That Can Be Protected by Host-Guest Interaction against Fast Back Electron Transfer

Characterization of the Guest Molecules

by **Rudolf Frank*** and **Hermann Rau**

Universität Hohenheim, Institut für Chemie 130, Garbenstrasse 30, D-70599 Stuttgart

Dedicated to Professor *André M. Braun* on the occasion of his 60th birthday

Anthraquinone and viologen moieties were combined to dyadic molecules with two redox centers. These dyades and their constituents were used as acceptors in photo-induced electron-transfer reactions. The experiments show that a caveat is necessary if one tries to derive the properties and the reactions of the dyades from those of their constituents: the spectral properties appear to be independent superpositions of those of the constituents. However, the redox potentials of the two redox centres in the dyades deviate from that of their constituents, the methylene bridge can not suppress a considerable interaction between the two redox centres. This is especially true when the redox potentials of the constituents are close to one another. From the quenching experiments, it can be concluded that electrolyte cations like Na^+ are engaged in the transition states of the electron-transfer reactions. In this way, they can control the fate of the transferred electron.

1. Introduction. – The permanent light-induced charge separation is realized in the natural photosynthesis systems. Like the natural systems, all biomimetic systems fight against fast back electron transfer under conversion of the photon energy to heat within the system. One type of such a system is represented by the polyades, molecules in which a light-absorbing unit and several quenchers with suitable redox potentials are more or less rigidly connected covalently. The aim is the local separation of the electron and the hole, and an increase in lifetime before recombination of the two. Efforts to construct biomimetic polyades and dyades with redox centers separated by large distances were successful, lifetimes of such intramolecular ion pairs can reach several hundred microseconds [1][2].

On the other hand, the distance of the electron-hole pair in polyades is limited by the dimensions of the polyade. This approach neglects the chance of diffusion apart of the reduced and oxidized molecule, which is an asset of the intermolecular electron transfer. Another concept is the combination of the advantages of both approaches. The idea is to use a dyadic quencher in which one part accepts the electron from an excited donor and funnels it to the other part which is protected from contact with the remaining oxidized donor. This may be achieved by means of a host molecule that includes that part of the dyade molecule that finally carries the transferred electron. So, in fact, the quenching unit is like a straw-protected Chianti-vine bottle with the antenna part of the dyade molecule sticking out of the protecting host and the electron-storing part inside.

In this paper, we report, as a first step, the synthesis of two quencher dyades, **MV²⁺AQ** and **DM²⁺AQ**, their redox properties, their transients on quenching of exited tris(2,2′-bipyridine-κN^1,$\kappa N^{1'}$)ruthenium(2 +) ([Ru(bpy)₃]²⁺) complexes (*Rubpy), and we compare them to the two constituents. We find several reduction steps by electrochemical and spectroscopic observation, identify the dyade unit that quenches preferentially, observe the transients of the reduced dyade radical, and identify that part of the dyade carrying the transferred electron. We further show that, by changing the reaction conditions, it is possible to control to which part of these dyades the electron is preferentially transferred.

DM²⁺AQ R = CH₃

MV²⁺AQ R = H
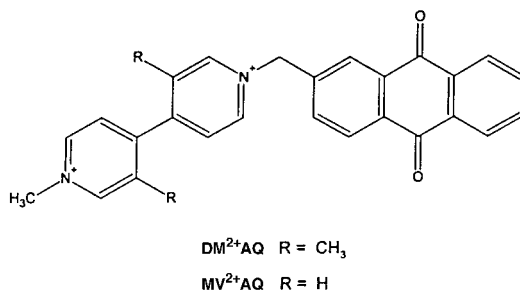
First experiments with β-cyclodextrin as a host are also reported. These results of encapsulation in β-cyclodextrin reveal the need to search for a better host.

2. Experimental. – 2.1 *Materials*. Acetonitrile (MeCN) for DNA synthesis from *Roth*, Et₄NClO₄, NaClO₄, and NaNO₃ from *Fluka* or *Aldrich*, iodomethane, 4,4′-bipyridine from *Aldrich*, and 2-(bromomethyl)anthra-quinone (= 2-(bromomethyl)anthracene-9,10-dione; *purum*) from *Fluka* were used without further purification. The 2-methylanthraquinone (= 2-methylanthracene-9,10-dione; **MAQ**) from *Fluka* and methylviologen (= 1,1′-dimethyl-4,4′-bipyridinium; **MV²⁺**) dichloride hydrate from *Aldrich* were recrystallized several times from EtOH or H₂O resp. The 3,3′-Dimethyl-4,4′-bipyridine (**DM**) was synthesized according to the method of *Stoehr* and *Wagner* [3][4]. The synthesis of the dyades, consisting of the combination of 2-(bromomethyl)anthraqui-none and the two different bipyridines, was performed similarly to that described by *Willner* and co-workers [5]. Instead of EtOH – as in [5] – we dissolved the educts in toluene. The advantage of this method is that the monoalkylated bipyridines immediately precipitate from the soln. The methylations with iodomethane at the second N-atom again were performed according to [5]. To transform the resulting iodide or bromide salts to perchlorates, they were dissolved in the minimum amount of H₂O. When these solns. were mixed with sat. NaClO₄ solns., the perchlorates of **MV²⁺AQ** or **DM²⁺AQ** precipitated. By the same methods, **DM** was alkylated with iodomethane to finally yield 1,1′,3,3′-tetramethyl-4,4′-bipyridinium (**DMV²⁺**) perchlorate.

2.2 *Electrochemical Measurements*. Most experiments were performed at salt concentrations of 0.1 mol l⁻¹. Redox potentials (half-wave potentials) were determined by the differential-pulse (DP) technique as described earlier [6][7]. Electrochemical reduction of **MV²⁺AQ** and **DM²⁺AQ** in optically transparent thin-layer cells (OTTL) has been described earlier, too [6][7]. Whereas these measurements and all DP measurements could be performed in pure MeCN, the electrochemical reduction of **DMV²⁺** in OTTL cells at a gold-grid electrode needed the addition of H₂O, at least to a volume fraction of 5%. The OTTL cell used for these measurements was almost identical to that of *Watanabe* and *Honda* [8]. This OTTL was placed in the sample compartment of a *Cary-50* spectrophotometer.

2.3 *Quenching Experiments*. If not stated otherwise, all experiments were performed in MeCN. Exper. details are given in [6][7].

3. Results and Discussion. – During early investigations of the dyades, it was found that their properties can be understood only on the basis of the properties of their constituent parts. Those of **MV²⁺** and **MAQ** are published [9][6][7], those of **DMV²⁺** as

well as those of the dyades are presented in this work. The influence of Et_4NClO_4 and $NaClO_4$ is used for fine tuning of the redox properties and to control the fate of the transferred electron.

3.1. *Spectra and Redox Potentials of the Molecules in Different Oxidation States*. The spectra of the dyades **MV²⁺AQ** and **DM²⁺AQ** are the same as the sum of the spectra of the constituent molecules, indicating virtual electronic insulation of the constitutent parts. Within experimental errors, this also holds for the partially reduced species **MV⁺AQ**, **DM⁺AQ**, and **DM²⁺AQ⁻**. Therefore, the transient concentrations of these species in quenching experiments can be determined from the absorption coefficients of **MV⁺** (λ_{max} 610 nm, ε_{max} 13 900 l mol⁻¹ cm⁻¹), **DMV⁺** (λ_{max} 776 nm, ε_{max} 13 800 l mol⁻¹ cm⁻¹) [10], and **MAQ⁻** (λ_{max} 539 nm, ε_{max} 10 312 l mol⁻¹ cm⁻¹).

A survey of the redox potentials of **MAQ**, **MV²⁺**, and **MV²⁺AQ**, and of **MAQ**, **DMV²⁺**, and **DM²⁺AQ** in MeCN is given in *Figs. 1,a* and *b*. The numbers for the redox potentials, which are primarily important for the quenching experiments, are compiled in *Table 1*. In the center column of *Fig. 1,a* and *b*, the values of the redox potentials of the constituents **MV²⁺** and **DMV²⁺** are shown; these values are not sensitive to the electrolyte type. The columns immediately to the left and right show the data of **MAQ**. As reported earlier, its redox potential is sensitive to the kind of electrolyte. The reason for this behavior is association of **MAQ⁻** with Na⁺ [6][7]. In the extreme left and right columns, the redox potentials of the dyades are shown. It is obvious that, compared to **MV²⁺** and **MV²⁺AQ**, methyl substitution at the 3 and 3′ positions of the viologen lowers the redox potentials of both **DMV²⁺** and **DM²⁺AQ** by *ca.* 400 mV, which is due to the torsion of the central bond between the aromatic rings of the viologen unit. A unique property of the dyades is that they are reduced at less negative potentials than their constituting parts at almost all reduction levels. This shows that, whereas the methylene bridge is sufficient to decouple the optical properties of the constituents, it is not sufficient to keep their electrochemical properties separate.

With Et_4NClO_4 as a supporting electrolyte, the viologen centers are reduced first in both dyades. But, whereas the redox potential of the viologen part in **MV²⁺AQ** is not sensitive to the kind of the electrolyte, the redox behavior of the viologen part in **DM²⁺AQ** shows the same sensitivity to the kind of the electrolyte as the anthraquinone

Table 1. *Redox Potentials*. All data are valid for c(salt) = 0.1 mol l⁻¹. Redox potentials are reproducible within 10 to 20 mV. Data in the presence of $NaClO_4$ are given only for the data that deviate from those in the presence of Et_4NClO_4. ΔG^0_{23} values were calculated by means of $E_{1/2}$(Rubpy³⁺/*Rubpy²⁺) = −603 mV *vs.* SHE, w_p = −3.96 kJ mol⁻¹, and w_r = 5.28 kJ mol⁻¹

Redox couple		$E_{1/2}$ *vs.* SHE / mV	ΔG^0_{23} / kJ mol⁻¹
In the presence of Et_4NClO_4	**MAQ / MAQ⁻** [a])	− 742	9.44
	MV²⁺ / MV⁺ [b])	− 225	− 37.5
	DMV²⁺ / DMV⁺	− 615	− 0.16
	MV²⁺AQ / MV⁺AQ	− 161	− 44.0
	DM²⁺AQ / DM⁺AQ	− 566	− 4.9
In the presence of $NaClO_4$	**MAQ / MAQ⁻** [a])	− 649	7.6
	DM²⁺AQ / DM⁺AQ	− 501	− 11.2

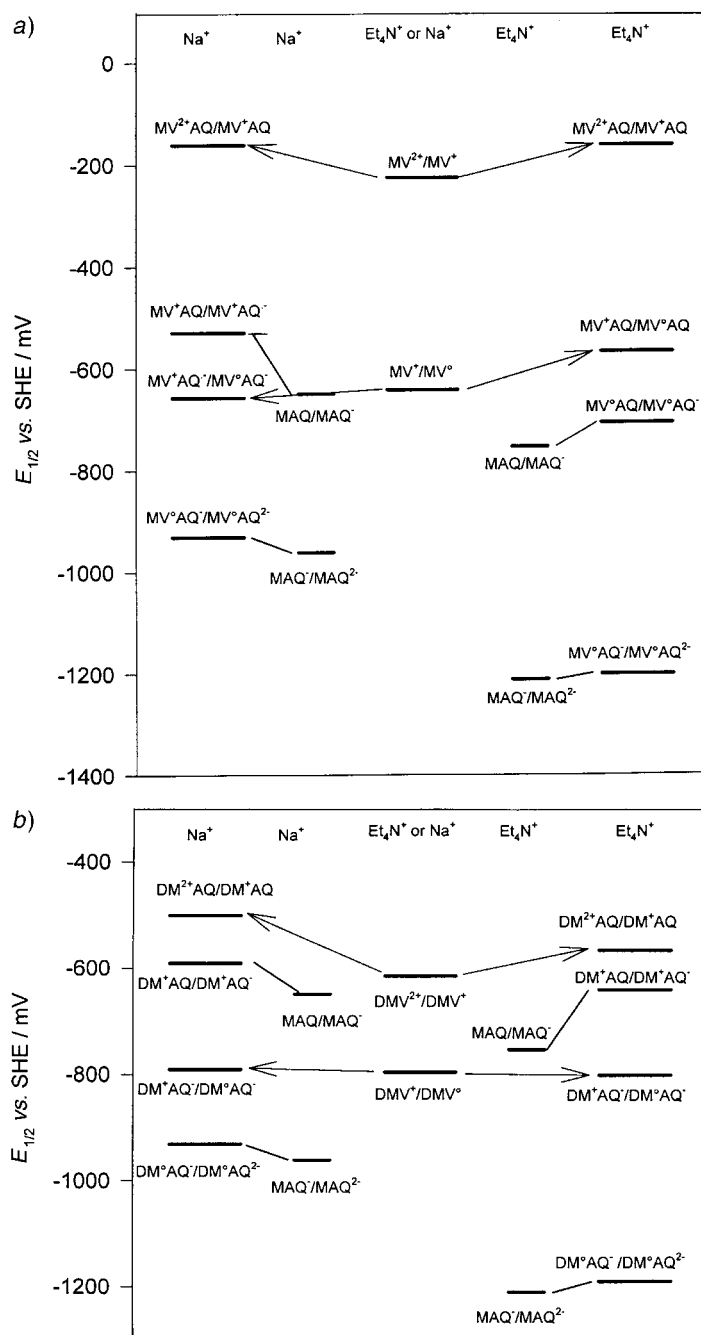[a]) Data from [6][7]. [b]) Data from [11].

Fig. 1. *Redox potentials of the various reduction states* a) *of the dyade* **MV²⁺AQ** *and* b) *of the dyade* **DM²⁺AQ** *in comparison to those of their constituents.* Left columns: supporting electrolyte is NaClO₄; right columns: supporting electrolyte is Et₄NClO₄.

constituent alone. It is obvious that this occurs preferentially when the difference of the redox potentials is small. Again, this means that the methylene bridge does not separate the electrochemical properties of the two constituents. At the moment, we have no model to rationalize these observations. Effects like these, however, should be present in polyades as well, especially when these polyades contain several redox centers with close-lying redox potentials intended for good energy conservation in electron-hole separation. To our knowledge, such effects have not yet been studied and reported.

The relationships between the redox potentials of the dyades and their constituents given in *Fig. 1* are in agreement with the information on chemical reduction from the spectra taken in OTTL cells. In the case of $MV^{2+}AQ$, measurements in OTTLs show that the electron is transferred to the viologen part only, and it remains there. In the case of $DM^{2+}AQ$, the results are not as clear as suggested by *Fig. 1*. OTTL Measurements indicate that in the presence of Et_4N^+ as well as Na^+, the reduction $DM^{2+}AQ \rightarrow DM^+AQ$ is the main process. But, as will be seen later in transient measurements, too, the reduction $DM^{2+}AQ \rightarrow DM^{2+}AQ^{\cdot-}$ cannot be excluded in the presence of Na^+. We cannot decide from OTTL experiments whether $DM^{2+}AQ^{\cdot-}$ is formed by direct electrolysis at the electrode or by intra- or intermolecular charge transfer between the constituents of the dyades. So the reduction $DM^{2+}AQ \rightarrow DM^+AQ$ should be regarded as the main but not the only process.

In addition, reduced species like $DM^{2+}AQ^{\cdot-}$ appear to be unstable on the electrochemical timescale, as has already been observed during the electrochemical reduction of MAQ in OTTL cells in the presence of Na^+.

3.2. *Quenching Experiments.* Electron quenching is assumed to occur according to the well-accepted *Scheme*, which defines the rate constants k_{ij} and the reacting species: **PC** precursor complex, **CI** contact ion pair, **FI** free ions.

Scheme

The quenching of the emission of excited Rubpy by MV^{2+}, DMV^{2+}, and the dyades is very sensitive to ionic strength. This is shown in *Fig. 2,a* and *b*. The steep rise at low ionic strength is due to the expressed change of electrostatic interactions. At ionic strengths higher than 0.1 mol l^{-1}, these changes become small, and their effect is approximately balanced by the change in viscosity. Thus, the observed values of k_q show

the same behavior as for the diffusion-controlled rate constants. The diffusion-controlled rate constants show a steep rise from $(0.29$ to $1.21) \cdot 10^{10}$ l mol^{-1} s^{-1} when the ionic strength is changed from 0 to 0.1 mol l^{-1}, reach a flat maximum $(1.45 \cdot 10^{10}$ l mol^{-1} s$^{-1})$ at 0.3 mol l^{-1}, and decrease to $1.40 \cdot 10^{10}$ l mol^{-1} s^{-1} at 0.5 mol l^{-1}. Therefore, most of the measurements were performed at ion strength 0.1 mol l^{-1} only. The quenching behaviour of the dyades and that of the constituting molecules shown in *Fig. 2* again suggests that the viologen part of the dyade in all cases accepts the electron from the *Rubpy. Although the nature of the cation of the supporting electrolyte changes the redox potentials [6][7] and ΔG^0 (*e.g.* for **DM^{2+}AQ**: $\Delta G^0 = -5$ kJ/mol in the presence of Et$_4$ClO$_4$, $\Delta G^0 = -11$ kJ/mol in the presence of NaClO$_4$), this has no strong effect on the quenching constants. **MV^{2+}AQ** is a slightly better quencher than **MV^{2+}**, an observation that corresponds to the change of ΔG^0_{23}. A surprising result is the extremely weak quenching ability of **DMV^{2+}** (open and solid triangles in *Fig. 2,b*), which is independent of the kind of electrolyte and comparable to the **MAQ**s, and the expressed rise of the quenching rate constant from $0.035 \cdot 10^9$ to $2.5 \cdot 10^9$ when the **DMV^{2+}** and the anthraquinone are combined within the dyade. This observation as well as the electrochemical behavior suggests some strong interaction between the two redox centers in the dyade.

3.3. *Transients*. The transient absorption spectra of the dyades can be understood in part by using the spectra of the radical ions **MV$^+$**, **DMV$^+$**, and **MAQ$^-$**. The transient spectrum created with **MV^{2+}AQ** in the quenching reaction is identical with that of the extensively studied **MV$^+$**.

When **DMV^{2+}** is used as a quencher 2 μs after the laser flash, we get the spectrum shown in *Fig. 3*. This transient spectrum is identical with that of **DMV$^+$**, produced by electrochemical reduction and observed in OTTL cells. Whereas the transient spectra of **MV$^+$** disappears totally, the case of **DMV^{2+}** is more complicated. The **DMV$^+$** spectrum changes to a second transient spectrum with a maximum around 675 nm within approximately 100 μs. This spectrum persists for several 100 μs. A spectrum like this has first been interpreted as being due to the solvated electron in MeCN [12], later as an [MeCN$^-$ ⋯ MeCN] dimer [13]. However, the lifetime of this dimer is reported to be much smaller $(0.7-5$ μs) than that of our transient. We, therefore, cannot assign the second transient spectrum at present.

The same behavior and transient spectra are observed when **DM^{2+}AQ** is used as a quencher in the presence of Et$_4$NClO$_4$ as a supporting electrolyte. In the presence of NaClO$_4$, the course of this photo-induced electron-transfer reaction changes. The observed transient spectra reveal that both parts of the dyades can be reduced. *Fig. 4,a* and *b*, show that increasing concentrations of NaClO$_4$ cause the fraction of **DM$^+$AQ** to decrease and the fraction of **DM^{2+}AQ$^-$** to increase.

When we used **MAQ** as a quencher, we observed the transient spectrum of the **MAQ$^-$** radical anion at 535 nm in the presence of Et$_4$NClO$_4$ and at 515 nm in the presence of NaClO$_4$. This shift is due to association of the **MAQ$^-$** radical anions with Na$^+$ cations [6][7]. When **DM^{2+}AQ** is used as a quencher, the presence of NaClO$_4$ enhances the probability of the **AQ** part of the dyade to be reduced. But, contrary to the behavior of **MAQ$^-$**, no corresponding shift of the transient absorbance to shorter wavelengths occurs. So we observe the puzzling situation that NaClO$_4$ obviously controls the course of the electron-transfer reaction, but spectroscopic measurements
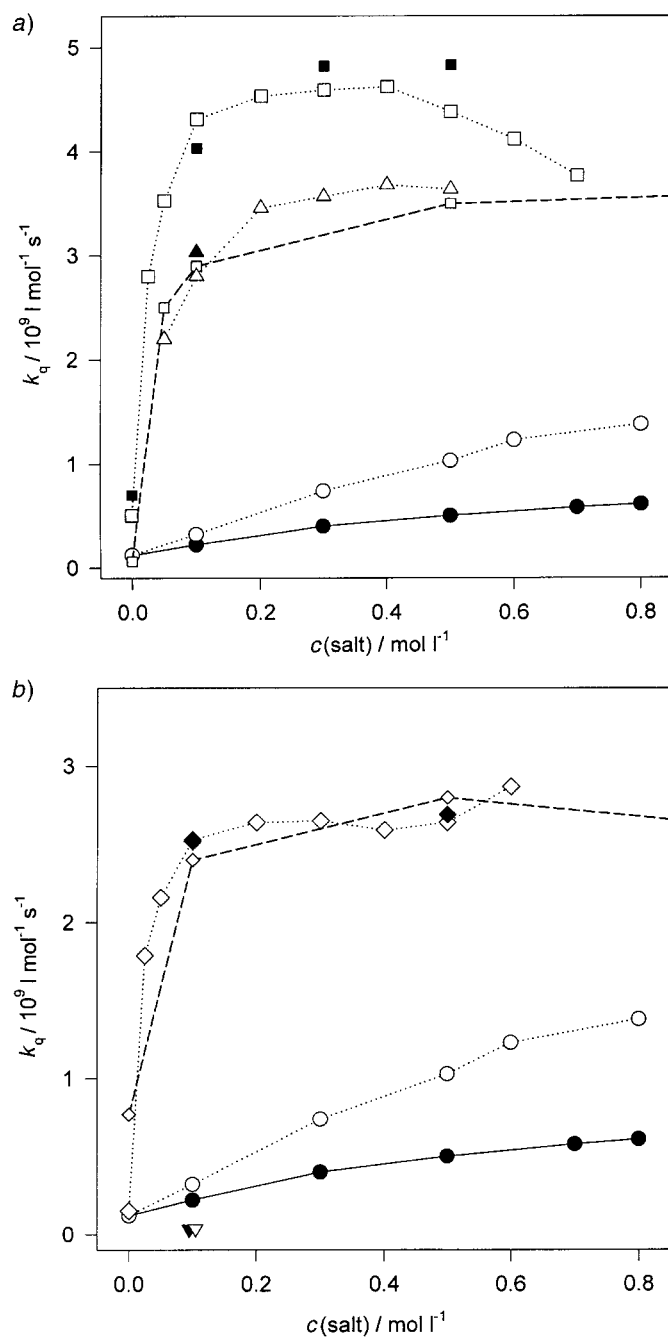
Fig. 2. *Quenching rate constants* a) *of the dyade* **MV²⁺AQ** *and* b) *of the dyade* **DM²⁺AQ** *and those of their constituents at various concentrations of Et₄NClO₄ and NaClO₄.* -●-, **MAQ** /Et₄NClO₄; ···○···, **MAQ** / NaClO₄; ■, **MV²⁺AQ** / Et₄NClO₄; ···□··· **MV²⁺AQ** / NaClO₄; --□--, **MV²⁺AQ** / NaNO₃, solvent H₂O; ▲, **MV²⁺**/Et₄NClO₄; ···△···, **MV²⁺** / NaClO₄; ◆, **DM²⁺AQ** / Et₄NClO₄; ···◇···, **DM²⁺AQ** / NaClO₄; --◇--, **DM²⁺AQ**/NaNO₃, solvent H₂O; ▼, **DMV²⁺** / Et₄NClO₄; ▽, **DMV²⁺** / NaClO₄.
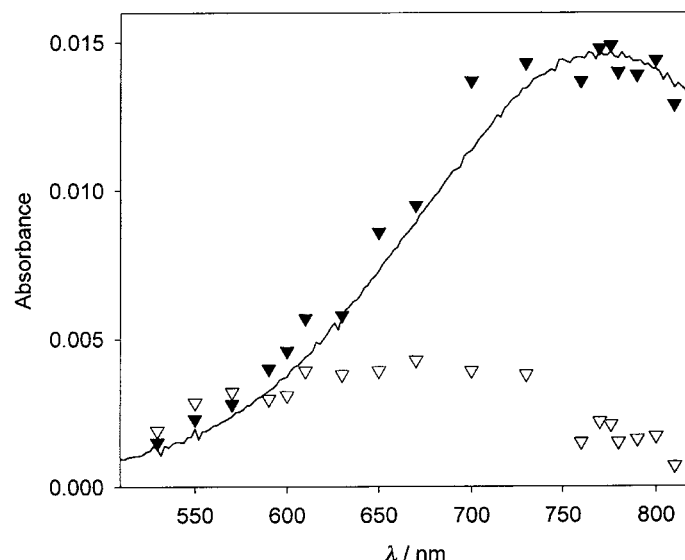
Fig. 3. *Transient spectra from *Rubpy /* **DMV²⁺** *quenching experiments.* ▼, Transient absorbance 2 μs after the laser flash; ▽, transient absorbance 120 μs after the laser flash; —, spectrum of **DMV⁺** adapted from OTTL measurements.

show that there is not much interaction between the products (**DM²⁺AQ⁻**) of the photo-induced electron-transfer reaction and Na⁺ cations. Bearing in mind the results of the electrochemical measurements, we have to state that Na⁺ cations are engaged in the transition states of the various electron-transfer reactions but not necessarily in the final states. Thus, it appears that Na⁺ can control the fate of the transferred electron if ΔG^0 of the corresponding reaction is small.

3.4. *Quantum Yields and* Marcus *Behavior.* The quantum yield of radical-ion production is defined as the ratio of the radical concentration and the concentration of the excited *Rubpy species. The former is taken from the transient spectra, the latter calculated from the flash profile and the absorbance of the solution according to a recently developed method [14]. (In short: To calculate the concentration changes due to light absorption from the laser flash and return of *Rubpy to the ground state, the volume of the cuvette is divided into 10^3 intervals. The changes within these intervals throughout the duration of the laser flash are calculated consecutively. To perform these calculations, the laser flash needs to be divided into suitable time intervals. Various methods have been tested with respect to exactness and calculation time.) Due to the bimolecular process, the fractions $c(\mathbf{DMV^+})/c(*\text{Rubpy})$, $c(\mathbf{MV^+AQ})/c(*\text{Rubpy})$, and $c(\mathbf{DM^+AQ})/c(*\text{Rubpy})$ depend on the concentration of the quenchers, but they approach a constant value when every *Rubpy can meet a quencher molecule within its lifetime, *i.e.* in the case of complete quenching. For *Rubpy, this can occur at quencher concentrations above 10^{-3} mol l⁻¹. Because of the restricted solubility of the dyades quantum yields were determined at quencher concentrations of $2 \cdot 10^{-3}$ mol l⁻¹, the results are compiled in *Table 2*.
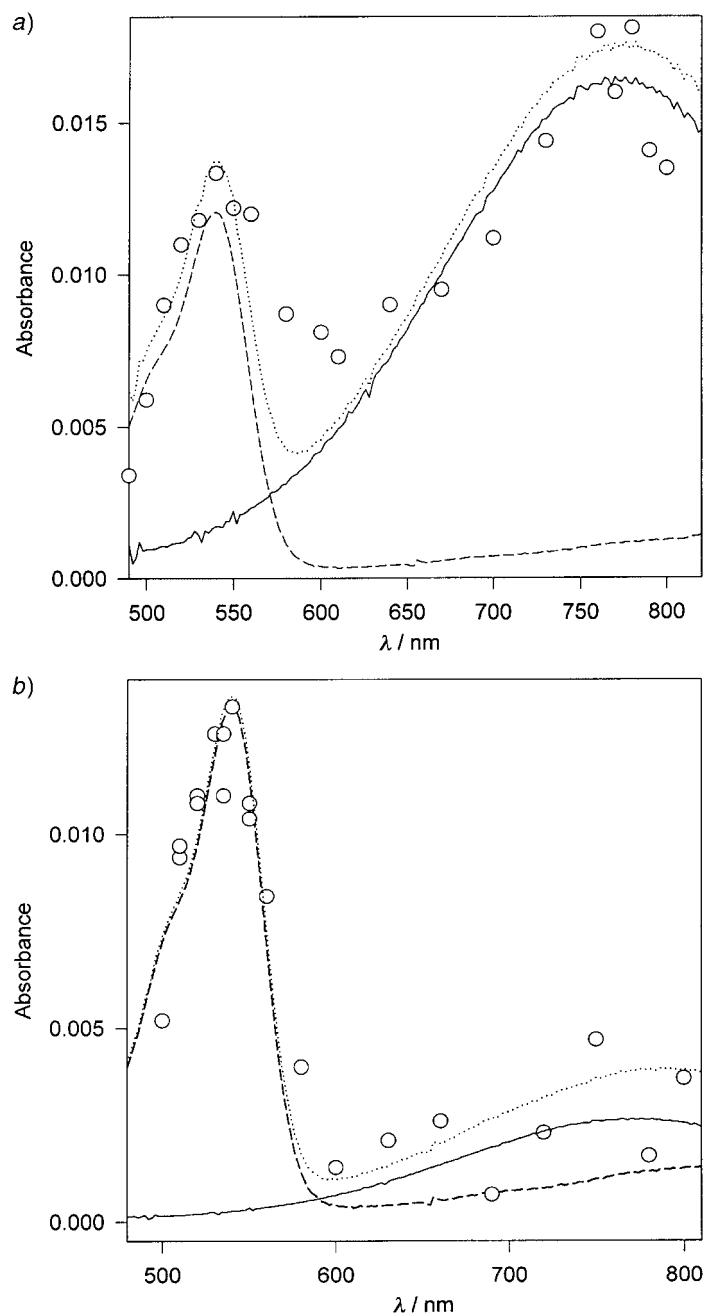
Fig. 4. *Transient spectrum from* *Rubpy / **DM²⁺AQ** *quenching experiments at* a) c*(NaClO₄) = 0.1 mol l⁻¹ and* b) c*/NaClO₄) = 0.5 mol l⁻¹.* ○ Transient absorbance, —, absorption spectrum of **DMV⁺** adapted from OTTL measurements; - - -, absorption spectrum of **MAQ⁻** adapted from OTTL measurements; · · · · ·, sum of **DMV⁺** and **MAQ⁻** spectra.

Table 2. *Quantum Yields at* c*(Quencher)* $= 2 \cdot 10^{-3}$ *mol* l^{-1}

Electrolyte (c/mol l^{-1})	φ (**MV$^+$AQ**)/%	φ (**DMV$^+$**)/%	φ (**DM$^+$AQ**)/%	φ (**DM^{2+}AQ$^-$**)/%
Et$_4$NClO$_4$ (0.1)	10.5 ± 2	2.7 ± 0.7	5.2 ± 0.7	< 0.5
NaClO$_4$ (0.1)	8.8 ± 2	< 1	2.5 ± 0.7	2.5 ± 0.7
NaClO$_4$ (0.3)			2.3 ± 0.7	3.3 ± 0.5
NaClO$_4$ (0.5)			< 0.5	3.3 ± 0.7

Whereas the quenching rate constants of the various species differ by several orders of magnitude, the quantum yields are rather close to each another. An analogous situation has been observed in a series of anthraquinones [7]. For light conversion systems this means that low quenching rate constants – caused by small ('photon energy saving') ΔG^0_{23} values – are not always a severe drawback. Low electron-transfer rate constants can be compensated by high quencher concentrations. However, given that every sensitizer meets a quencher and that k_{23} is not very low, the maximum quantum yield essentially is determined by the ratio $k_{34}/(k_{\mathrm{b}} + k_{34})$.

The quenching constant derived for the *Scheme* in a steady-state approximation is given by *Eqn. 1*. For the assessment of the complete electron-transfer process, we determine the individual rate constants. In brief, the rate constants k_{12}, k_{21}, and k_{34} can be calculated according to commonly accepted methods [15][16], k_{23} and k_{32} are connected by ΔG^0_{23}, and with the information about the quantum yield φ of total quenching, we have the ratio of $k_{34}/(k_{\mathrm{b}} + k_{34})$. (If k_{23} is very low, *e.g.*, in a system with near-zero or small positive $\Delta \mathrm{G}^0_{23}$, the rate constants need to be determined by an iterative, recently developed procedure [14].) In principle, the data show *Marcus* behavior. *Fig. 5* shows that the forward and back electron-transfer rate constants k_{23} and k_{b} of the dyades fit into the pattern of those of their constituent parts and some additional anthraquinone species studied earlier [6][7].

$$k_{\mathrm{q}} = \frac{k_{12}k_{23}(k_{\mathrm{b}} + k_{34})}{k_{21}k_{32} + k_{21}(k_{\mathrm{b}} + k_{34}) + k_{23}(k_{\mathrm{b}} + k_{34})} \tag{1}$$

3.5. *Activation Parameters*. In earlier studies with **MAQ**, one of the constituents of the dyades, we observed negative activation enthalpies. The activation parameters compiled in *Table 3* show that **DMV^{2+}** and the dyades yield normal, positive enthalpies of activation. This observation can be taken as a clue that, in all quenching reactions of the dyades, the viologen part is engaged, even when the electron finally rests on the anthraquinone part.

3.6. *Association of* **MV^{2+}AQ** *with* β-*Cyclodextrin in Water*. The cyclodextrin inclusion complexes have to be prepared in H$_2$O. It can be assumed that the more hydrophobic part of the dyade, *i.e.* the **AQ** part, is included in the host cavity. By mixing solutions of **MV^{2+}AQ** and β-cyclodextrin in spectroscopic tandem absorption cells, the association constant was determined from absorbance measurements according to *Benesi* and *Hildebrand* [17]. For **MV^{2+}AQ**, we obtained $K_{\mathrm{ass}} = 610 \pm 90$ l/mol. For comparison: the less hydrophobic 'anthraquinone-2-sulfonic acid' ($=$ 9,10-dihydro-9,10-dioxoanthracene-2-sulfonic acid) gave $K_{\mathrm{ass}} = 225 \pm 95$ l/mol.
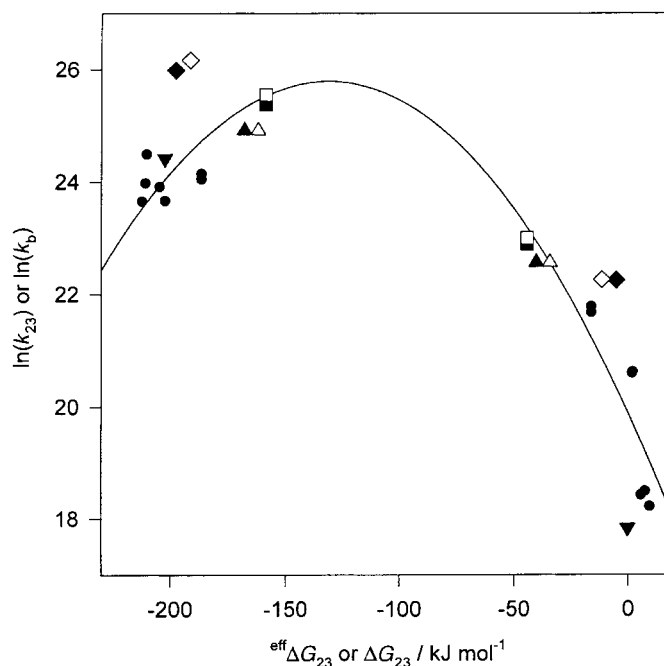
Fig. 5. *The ln(k$_{23}$) and ln(k$_b$) of the dyades and that of their constituents at* c*(salt) = 0.1 mol l^{-1}.* ■, **MV^{2+}AQ** / Et$_4$NClO$_4$; □, **MV^{2+}AQ** / NaClO$_4$; ◆, **DM^{2+}AQ** / Et$_4$NClO$_4$; ◇, **DM^{2+}AQ** / NaClO$_4$; ▲, **MV^{2+}** / Et$_4$NClO$_4$; △, **MV^{2+}** / NaClO$_4$; ▼, **DMV^{2+}** / Et$_4$NClO$_4$. ●, Data of all anthraquinone derivatives (2-methyl, 1-chloro, and 1-nitro) studied in [6][7] for comparison; in these studies, it was necessary to replace the ΔG$_{23}$ determined from electrochemical measurements by an effective *Gibbs* energy ^{eff}ΔG$_{23}$; this quantity is used here, too.

Table 3. *Activation Parameters of the Quenching Reactions at 25°*

Species // salt, c / mol l^{-1}	$\Delta H^{\pm}$ / kJ mol^{-1}	$\Delta S^{\pm}$ / J mol^{-1} K^{-1}	$\Delta G^{\pm}$ / kJ mol^{-1}
MV^{2+}AQ // Et$_4$NClO$_4$, 0.1	6.0 ± 2	-40 ± 7	18.1 ± 4.1
MV^{2+}AQ // NaClO$_4$, 0.1	5.7 ± 0.7	-41 ± 3	17.9 ± 1.6
DM^{2+}AQ // Et$_4$NClO$_4$, 0.1	5.7 ± 0.6	-46 ± 2	19.4 ± 1.2
DM^{2+}AQ // NaClO$_4$, 0.1	4.1 ± 1.3	-51 ± 5	19.0 ± 2.8
DM^{2+}AQ // NaClO$_4$, 0.5	5.0 ± 1.6	-47 ± 5	19.1 ± 3.1
DMV^{2+} // Et$_4$NClO$_4$, 0.1	7.3 ± 1	-76 ± 2	30 ± 1.6
DMV^{2+} // NaClO$_4$, 0.1	6.8 ± 1	-77 ± 5	29.8 ± 2.5
MAQ // Et$_4$NClO$_4$, 0.1 [a])	-17.6	-142	25.3
MAQ // NaClO$_4$, 0.5 [a])	-6.7	-95	21.7

[a]) Data from [6][7].

These results are reasonable, but the experiments caused some problems. After mixing, constant absorbance readings are reached only after a considerable time between 1 and 20 min. This is by orders of magnitude larger than the rate constants frequently observed for the dynamics of the host-guest interaction [18]. Moreover, this induction time is concentration-dependent, and the reproducibility is limited. It should

be mentioned that such induction times were also seen in NMR experiments which were conducted to test which part of the dyade is in the cavity of the cyclodextrin. These preliminary experiments show that extended experiments are necessary to find a host which in photo-induced electron-transfer experiments is as protective as the straw basket in the case of the Chianti-vine bottle.

REFERENCES

[1] D. Gust, T. A. Moore, A. L. Moore, *Acc. Chem. Res.* **1993**, *26*, 198.
[2] M. N. Paddon-Row, *Acc. Chem. Res.* **1994**, *27*, 18.
[3] C. Stoehr, M. Wagner, *J. Prakt. Chem.* **1893**, *48*, 1.
[4] G. Dörr, 'Rutheniumkomplexe und Zinnporphyrine als Sensibilisatoren in der photochemischen Wasserspaltung', Diploma Thesis, Universität Saarbrücken, 1985.
[5] I. Willner, J. Rosengaus, Y. Eichen, *New. J. Chem.* **1991**, *15*, 55.
[6] R. Frank, H. Rau, *Recl. Trav. Chim. Pays-Bas* **1995**, *114*, 556.
[7] R. Frank, G. Greiner, H. Rau, *Phys. Chem. Chem. Phys.* **1999**, *1*, 3481.
[8] T. Watanabe, K. Honda, *J. Phys. Chem.* **1982**, *86*, 2617.
[9] M. Z. Hoffmann, F. Bolletta, L. Moggi, G. L. Hug, *J. Phys. Chem. Ref. Data* **1989**, *18*, 219.
[10] See also N. A. McAskill, *Aust. J. Chem.* **1984**, *37*, 1579.
[11] H. J. Orthwein, 'Temperatur und Umgebungsabhängigkeit der Fluoreszenzlöschung von Rutheniumkomplexen durch Methylviologen', Diploma Thesis, Universität Hohenheim, 1988.
[12] A. Singh, H. D. Gesser, A. R. Scott, *Chem. Phys. Lett.* **1968**, *2*, 271.
[13] U. Schindewolf, *Angew. Chem.* **1978**, *90*, 939; T. Truon, *J. Phys. Chem.* **1982**, *77*, 5375; R. Boch, M. K. Whittlesey, J. C. Scaiano, *J. Phys. Chem.* **1994**, *98*, 7854; Y. Hirata, N. Mataga, *J. Phys. Chem.* **1983**, *87*, 1680.
[14] R. Frank, H. Rau, *EPA News Lett.* **1999**, *65*, 39.
[15] N. Kitamura, H. B. Kim, S. Okano, S. Tazuke, *J. Phys. Chem.* **1989**, *93*, 5750.
[16] C. Chiorboli, M. T. Indelli, M. A. Rampi-Scandola, F. Standola, *J. Phys. Chem.* **1988**, *92*, 156.
[17] J. H. Hildebrand, H. A. Bensi, *J. Am. Chem. Soc.* **1949**, *71*, 2703.
[18] M. L. Bender, M. Komiyama, 'Cyclodextrin Chemistry', Springer Verlag, Berlin-Heidelberg-New York, 1978.